Radiative Effects of Cloud Horizontal Inhomogeneity and Vertical Overlap Identified from a Monthlong Cloud-Resolving Model Simulation

XIAOQING WU

Department of Geological and Atmospheric Sciences, Iowa State University, Ames, Iowa

XIN-ZHONG LIANG

Illinois State Water Survey, Illinois Department of Natural Resources, and University of Illinois at Urbana–Champaign, Champaign, Illinois

(Manuscript received 12 November 2004, in final form 19 March 2005)

ABSTRACT

The representation of subgrid horizontal and vertical variability of clouds in radiation schemes remains a major challenge for general circulation models (GCMs) due to the lack of cloud-scale observations and incomplete physical understanding. The development of cloud-resolving models (CRMs) in the last decade provides a unique opportunity to make progress in this area of research. This paper extends the study of Wu and Moncrieff to quantify separately the impacts of cloud horizontal inhomogeneity (optical property) and vertical overlap (geometry) on the domain-averaged shortwave and longwave radiative fluxes at the top of the atmosphere and the surface, and the radiative heating profiles. The diagnostic radiation calculations using the monthlong CRM-simulated tropical cloud optical properties and cloud fraction show that both horizontal inhomogeneity and vertical overlap of clouds are equally important for obtaining accurate radiative fluxes and heating rates. This study illustrates an objective approach to use long-term CRM simulations to separate cloud overlap and inhomogeneity effects, based on which GCM representation (such as mosaic treatment) of subgrid cloud–radiation interactions can be evaluated and improved.

1. Introduction

Cloud systems often appear with distinct vertical overlap and inhomogeneity in their vertical and horizontal structures (e.g., Hahn et al. 1982, 1984). The representation of these systems and their interaction with radiation is one of the major uncertainties in general circulation models (GCMs). Studies have shown significant impacts of this subgrid cloud variability on the calculation of both shortwave and longwave radiative fluxes (e.g., Stephens 1984; Cahalan et al. 1994; Barker 1996; Liang and Wang 1997; Barker et al. 1999; Fu et al. 2000; Li and Barker 2002). Since complete observations of cloud systems are impossible and available measurements are very limited, the quantification of the effects of cloud inhomogeneity and vertical overlap is difficult.

Recent development of cloud-resolving models (CRMs) provides a unique opportunity to study this problem. The CRM-produced cloud condensate distributions have been increasingly used by the radiation community for various purposes. While GCMs require convection and cloud parameterizations, CRMs explicitly resolve convection and mesoscale organization, where cloud microphysical processes and cloud–radiation interactions directly respond to the cloud-scale dynamics. Wu and Moncrieff (2001) demonstrated that a CRM produces vertical and horizontal distributions of cloud liquid and ice that interact much more realistically with radiation than a GCM's single-column model (SCM), which calculates the radiative effect using a single volume of "effective" cloud properties. In most GCM parameterizations of cloud–radiation interactions, cloud liquid and ice water paths are assumed horizontally homogeneous and the vertical distribution of clouds is treated by cloud-overlap assumptions (e.g., Stephens 1984; Morcrette and Fouquart 1986; Gates 1992; Liang and Wang 1997). Consequently, the CRM simulation can get the top-of-the-atmosphere (TOA) and surface (SRF) net shortwave fluxes to agree simultaneously with observations from

Corresponding author address: Dr. Xiaoqing Wu, Iowa State University, 3010 Agronomy Hall, Ames, IA 50011.
E-mail: wuxq@iastate.edu

the Tropical Ocean Global Atmosphere (TOGA) Coupled Ocean–Atmosphere Response Experiment (COARE), whereas GCMs and SCMs generally fail to do so. Using the CRM simulation as a benchmark, Wu and Moncrieff (2001) estimated the radiative effect of subgrid cloud variability using the offline calculation of the radiative transfer model and showed that there is a strong impact of subgrid cloud variability on both shortwave and longwave radiative fluxes, which is consistent with other studies cited above.

In the present study, we further conduct a diagnostic analysis to quantify *separately* the effects of the overlap assumption and the subgrid horizontal variability of cloud optical properties on the radiative fluxes using the CRM-produced monthlong cloud-scale temperature, moisture, and condensate fields. We first introduce the CRM simulation, then describe the design of diagnostic experiment, and later quantify the effects of inhomogeneity and vertical overlap assumption on the top-of-the-atmosphere, surface radiative fluxes and radiative heating, followed by concluding remarks.

2. Cloud-resolving model simulation

The CRM is based on the Clark–Hall finite-difference formulation of the anelastic, nonhydrostatic equations (Clark et al. 1996). A Kessler (1969) bulk warm rain parameterization and a Koenig and Murray (1976) bulk ice parameterization are used. The radiation transfer parameterization is adopted from the National Center for Atmospheric Research (NCAR) Community Climate Model version 3 (CCM3; Kiehl et al. 1996). Effective radii of liquid and ice particles are assumed to be 10 and 30μm, respectively. The radiative effect of vertically varying partial cloudiness is represented in approximation to the random overlap assumption. In the shortwave radiation, this is approximated by modifying the cloud extinction optical depth as $\tau_c' = \tau_c A_c^{3/2}$, where A_c is the fractional cloud cover in the layer. The scaling was found to produce a result that is very close to the random overlap assumption, without the computational burden of doing the radiative transfer for the spectrum of all cloudy layer combinations. In the longwave radiation, the cloud emissivity ε_c is first accounted for by defining an effective cloud amount $A_c' = \varepsilon_c A_c$ in each layer; the probability of a cloud A_c' existing in a given layer concurrent with clear sky above or below this layer is then calculated following the random overlap assumption; and finally the radiation transfer is done once in the entire column by using the vertical profile of such probability. In both cases, the radiation calculations are performed every 150 s, with the most recent tendencies applied between consecutive calculations. The surface fluxes of sensible and latent heat are calculated using the observed sea surface temperature (SST) and a simplified version of the TOGA COARE surface flux algorithm (e.g., Wu et al. 1998).

The CRM domain is 900 km wide (300 columns with a horizontal grid spacing of 3 km) and 40 km deep (52 levels with a stretched grid, a 100-m increment at the surface and increasing to 1500 m at the model top). The lateral boundary conditions are periodic. Rigid, free-slip bottom and top boundary conditions are applied together with a gravity wave absorber in the uppermost 14 km of the domain.

The CRM is forced by the evolving large-scale advection of temperature and moisture over a 30-day period (5 December 1992–3 January 1993) during TOGA COARE. The analysis of the CRM simulation of tropical cloud systems and the comparison with observations can be found in Wu et al. (1998, 1999).

3. Description of diagnostic radiation calculations

Before presenting the results in the next section, two diagnostic calculations of radiative fluxes and heating rates are described here together with the CRM radiation calculation. Similar diagnostic calculations with the use of various CRM simulations have been adopted by increasing numbers of studies (e.g., Barker et al. 1999; Wu and Moncrieff 2001; Wu et al. 2002; Li and Barker 2002; Wu and Liang 2003; Stephens et al. 2004; Xu 2005). The full CRM approach (M0; Wu and Moncrieff 2001) uses binary clouds (i.e., completely overcast or clear sky) in each grid box at an individual level of every 3-km column. We define a grid box at a given level to be completely overcast if the sum of liquid and ice water path exceeds a threshold of 0.2 g m^{-2} or otherwise totally clear-sky. The radiative flux and heating are calculated for each column using the radiative transfer model, and the 300 columns are then averaged to get the mean radiative flux and heating for the domain. The radiative effect of subgrid cloud horizontal (inhomogeneity) and vertical (geometric) distribution is thereby explicitly included in the CRM-produced radiative fluxes and heating rates.

Wu et al. (2002) presented a diagnostic calculation M2 to estimate the impact of cloud inhomogeneity on the radiative fluxes using the cloud properties simulated by the CRM. For each completely overcast grid box at a given level, the cloud optical properties (including emissivity, extinction optical depth, single scattering albedo, asymmetry parameter, and forward scattered fraction), temperature and water vapor mixing ratio are replaced by the mean value over the cloudy

boxes at that level. So the 30-day mean vertical profile and standard deviation of cloud fraction are the same for M2 and M0 (Fig. 1). Because the cloud emissivity is an exponential function of cloud water path, the mean emissivity averaged over all 300 columns is different from that calculated using the 300-column mean cloud water path (Fig. 2). The standard deviation of domain average shows large spatial variation of emissivity between 3 and 12 km. Therefore, by conserving the cloud optical properties instead of cloud water path (e.g., Barker et al. 1999; Xu 2005) over the domain, the parameterization of cloud optical properties will not affect the difference between M2 and M0. As in M0, the radiative transfer is calculated for each column and the mean radiative fluxes and heating rates are obtained by averaging all 300 columns. The removal of inhomogeneity of temperature and moisture fields has negligible effect on the domain-averaged radiative fluxes (less than 0.5 Wm^{-2}). Thus the difference between M0 and M2 mainly represents the effect of cloud horizontal inhomogeneity.

In the diagnostic calculation M1 (Wu and Moncrieff 2001), the mean cloud optical properties, cloud fraction, temperature and moisture profiles are obtained from the 300 columns of the CRM domain, and then the radiative transfer is calculated once using the mean profiles. In this case, the cloud vertical distribution has to be treated by certain cloud-overlap assumptions (a random overlap assumption currently used in the CCM3 radiation scheme) because there is only one column for each time step. So M1 is the same as what a SCM or GCM does except the cloud amount and optical property profiles are averages from the CRM. Because the mean cloud optical properties are identical, the difference between M2 and M1 is due to the use of random overlap assumption. Note that M1 calculation is different from the random overlap calculation of Barker et al. (1999). Barker et al. applied random numbers to generate cloud distribution of all columns over the CRM domain and then conducted radiative transfer calculation in each column to obtain final domain-averaged fluxes and heating rates. The procedure of Barker et al. is similar to that used in the mosaic treatment of subgrid cloud variability (Liang and Wang 1997) for vertically independent clouds, where a very small set of columns are considered.

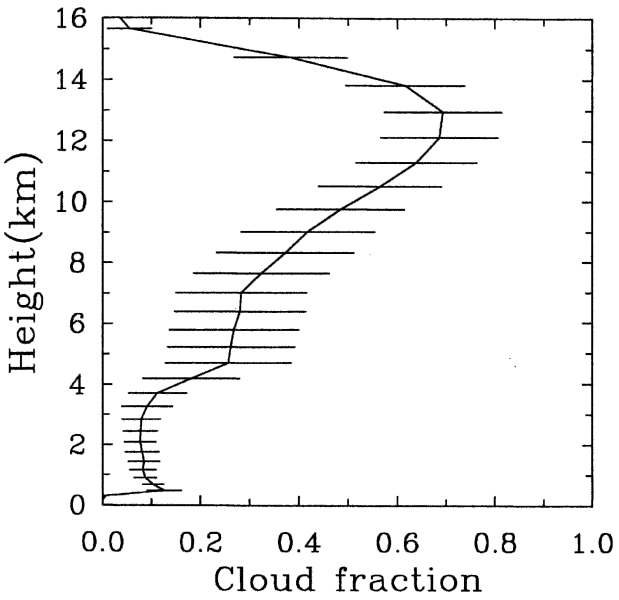

FIG. 1. The 30-day mean profile of cloud fraction for the CRM, and diagnostic radiation calculations M2 and M1. Horizontal bars are the standard deviations of 15-min cloud fraction, which show the temporal variability of cloud fraction during the 30-day period.

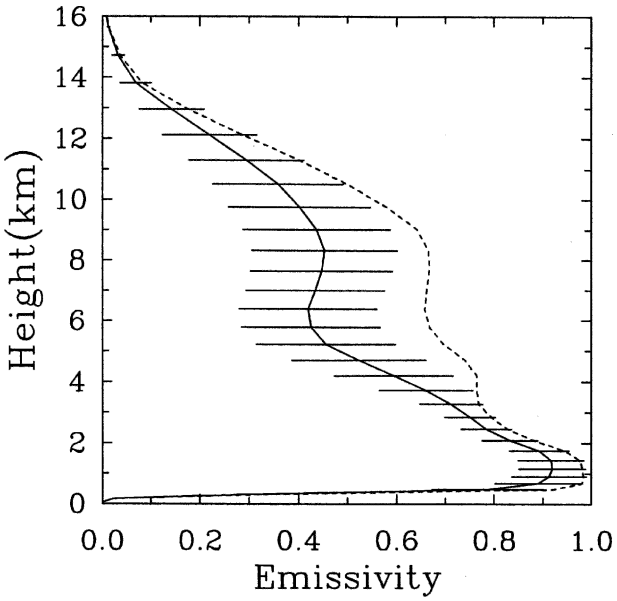

FIG. 2. The 30-day mean profiles of emissivity averaged over the 300 columns of the CRM domain (solid) and emissivity calculated using the domain-averaged cloud water path (dashed). Horizontal bars are the standard deviations of the domain-averaged emissivity, which show the spatial variability of emissivity during the 30-day period.

4. Effects of cloud horizontal inhomogeneity and vertical overlap

Table 1 shows the 30-day mean net longwave (LW) and shortwave (SW) radiative fluxes at the TOA and the surface (SRF). The SW flux differences between M0 and M2 are more than 30 W m^{-2} at both the TOA

TABLE 1. The 30-day (5 Dec 1992–3 Jan 1993) mean and standard deviation of longwave (LW) and shortwave (SW) radiative fluxes at the TOA and surface (SRF) from the CRM (M0) and diagnostic radiation calculations (M1 and M2).

	Mean			Deviation		
Flux (W m^{-2})	CRM M0	M2 (M0–M2)	M1 (M2–M1)	CRM M0	M2	M1
Q_{LW}(TOA)	−195.8	−182.6 (−13.2)	−171.2 (−11.4)	29.7	32.4	32.2
Q_{LW}(SRF)	−48.2	−46.4 (−1.8)	−39.3 (−7.1)	8.3	8.4	8.2
Q_{SW}(TOA)	274.8	243.6 (31.2)	238.4 (5.2)	39.0	46.4	50.7
Q_{SW}(SRF)	179.3	145.9 (33.4)	141.1 (4.8)	42.0	50.3	55.3

and SRF. The removal of cloud inhomogeneity in the horizontal domain enhances the SW reflection at the TOA, producing a smaller net flux. The increase in reflection at the TOA leads to less insolation to the surface, causing a smaller net flux at the SRF. This result indicates that the CCM3 scheme, like many GCM parameterizations of cloud–radiation interactions that assumes horizontally homogeneous cloud optical properties, will substantially underestimate the shortwave flux. The removal of cloud inhomogeneity also reduces the net longwave flux by more than 10 W m^{-2} at the TOA and about 2 W m^{-2} at the SRF. This suggests that more longwave radiation will be emitted to space if the subgrid-scale horizontal variability of cloud properties is included in GCM radiation parameterizations.

The cloud inhomogeneity effect can be further analyzed from the scatterplot of M0 versus M2 shown in Fig. 3. Each point represents a correspondence between the two domain-averaged fluxes in comparison at a 15-min sample during the 30-day period. If there is no inhomogeneity effect, all points should lie along the diagonal line. The interesting feature in these plots is that all points are below (above) the diagonal line with some points on the line for the shortwave (longwave) fluxes. This shows that without the subgrid-scale cloud variability the effect of cloud optical properties on domain-averaged fluxes is exaggerated. A number of schemes (e.g., Stephens et al. 1991; Calahan et al. 1994; Barker 1996; Li and Barker 2002) have included the effects of cloud inhomogeneity on shortwave and longwave fluxes by modifying within-cloud variance parameterizations. The CRM-produced 30-day-long cloud and radiative properties will be a useful dataset to evaluate these schemes.

Table 1 also lists the 30-day mean radiative fluxes from the diagnostic calculation M1. As explained in section 3, the cloud optical properties are averaged over the domain first and the domain-averaged flux is then obtained by a single radiative transfer calculation. The random overlap assumption is applied to represent the vertical distribution of clouds in the M1 radiation calculation unlike in M2, which explicitly resolves the vertical cloud structure. The random overlap assumption tends to overestimate the total cloud cover (e.g., Tian and Curry 1989), which results in smaller net TOA and SRF shortwave and longwave fluxes in M1 than M2. The 30-day mean M2 − M1 differences of TOA and SRF net shortwave fluxes (5.2 W m^{-2}) are much smaller than the M0 − M2 values (31.2 W m^{-2}). This suggests that the mean effects of random overlap assumption on the domain-averaged shortwave fluxes over the 30-day period are smaller than those of horizontal cloud inhomogeneity. On the other hand, the differences of longwave fluxes are comparable between the two at the TOA, whereas they are significantly enhanced in the M2 − M1 compared to M0 − M2 at the SRF. Given the strong dependence on vertical temperature structure, the longwave flux differences may induce significant feedbacks (e.g., Liang and Wang 1997) and consequently both cloud inhomogeneity and geometry effects are important.

Figure 4 shows the scatter plots of M1 versus M2, depicting a more comprehensive picture for the effects of the overlap assumption on the radiative fluxes. For the longwave fluxes, all points are above or on the diagonal line (Figs. 4c,d). The overlap assumption caused the systematic overestimation of cloud properties, which resulted in the blockage of more longwave radiation in M1 than in M2 during the entire 30-day period. The contrast is more profound at the SRF than TOA. For shortwave fluxes, the effect of the overlap assumption is mixed, where points spread around the diagonal line (Figs. 4a,b). Thus the random overlap assumption causes both overestimation and underestimation (points above and below the diagonal line) of total cloud optical properties during the 30-day period. This leads to smaller M2 − M1 differences of 30-day mean net TOA and SRF as compared to the M0 − M2 values (Table 1).

Figure 5 compares the 30-day mean profiles of shortwave, longwave and total radiative heating rates from the CRM and two diagnostic calculations. The comparison indicates the significant impact of cloud inhomogeneity and vertical overlap assumptions on the radiative

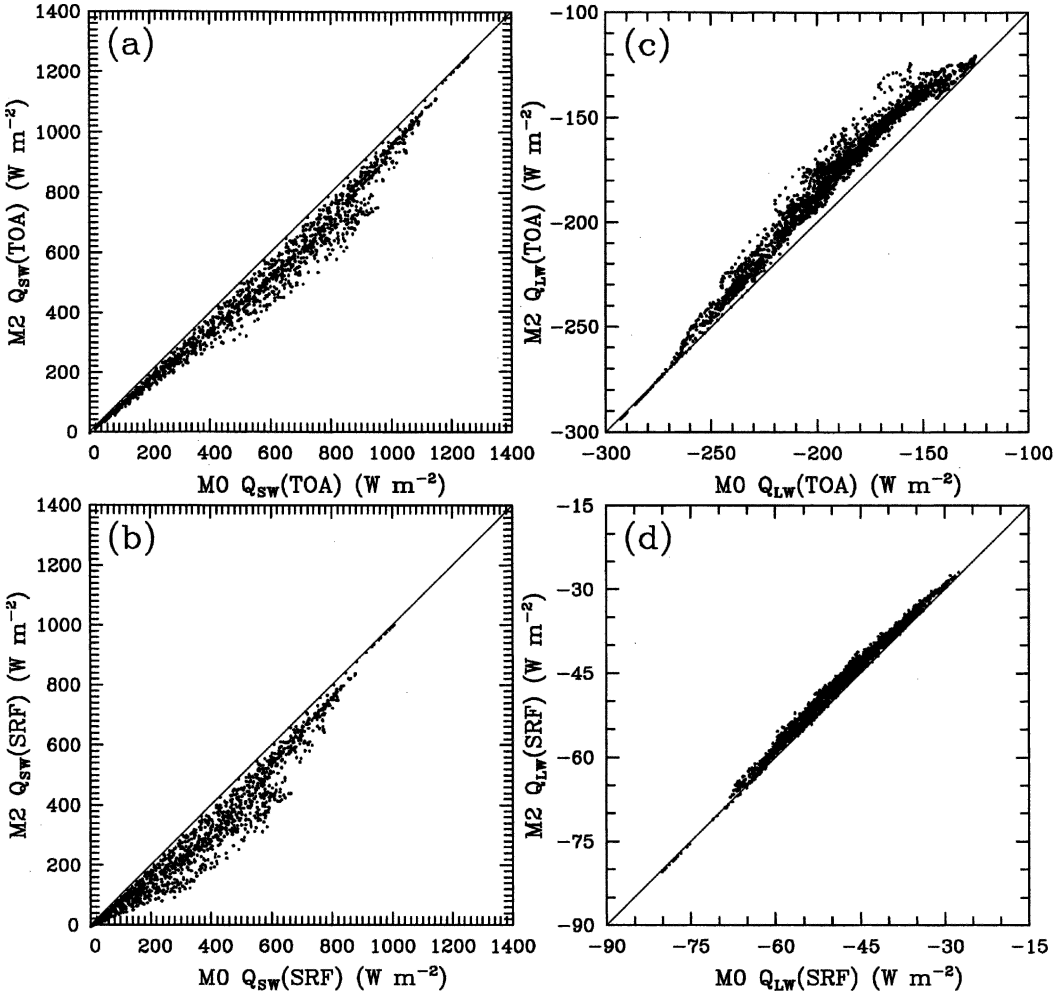

FIG. 3. Scatter diagrams of CRM (M0) vs diagnostic radiation calculation (M2) for net shortwave fluxes at (a) TOA and (b) SRF and net longwave fluxes at (c) TOA and (d) SRF. The dotted points represent 15-min samples.

heating rates. For M2, the removal of inhomogeneity enhances (reduces) the shortwave heating above (below) 8 km relative to M0 (Fig. 5a). The use of the random overlap assumption produces less shortwave heating in the upper (above 10 km) and lower (below 4 km) troposphere, and more heating in the middle troposphere (between 4 and 10 km) from M1 than those from M2 (Fig. 5a). The overlap assumption has relatively smaller impact on the mean shortwave heating profile compared to the inhomogeneity effect. For the longwave, the removal of inhomogeneity and the random overlap assumption increases (decreases) the cooling rate above (below) 9 km (Fig. 5b). The 30-day mean total radiative heating profile in the CRM (M0) is dominated by the longwave cooling rate (Fig. 5c). Without the cloud inhomogeneity, the cooling rate is reduced throughout all levels between 2 and 14 km. A net heating rate appears between 8 and 10 km. The random overlap assumption also reduces the cooling rate below 8 km, but enhances the cooling rate above.

5. Summary and concluding remarks

The representation of subgrid cloud–radiation interaction has been one of major challenges for the radiation parameterization in GCMs. Through the comparison of CRM with observations and SCM simulations of tropical cloud systems, Wu and Moncrieff (2001) showed a general agreement of radiative fluxes between the CRM and observation but large discrepancies in cloud condensates and radiative fluxes between the SCM and CRM. While the existence of large differences between the SCM and CRM indicated the problem in the SCM cloud parameterization, the diagnostic calculation M1 using the GCM radiation scheme and the CRM-produced cloud properties demonstrated

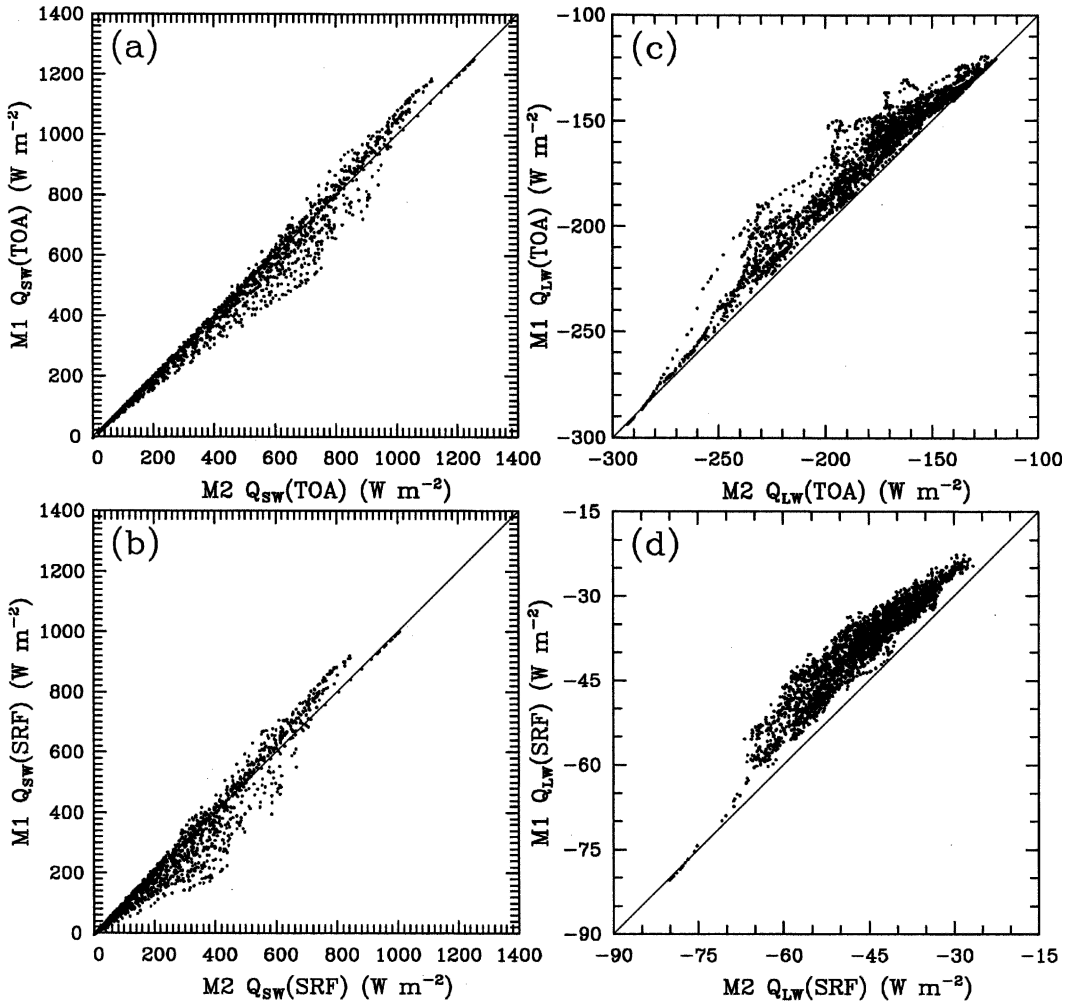

FIG. 4. Scatter diagrams of diagnostic radiation calculations M2 vs M1 for net shortwave fluxes at (a) TOA and (b) SRF and net longwave fluxes at (c) TOA and (d) SRF. The dotted points represent 15-min samples.

great impact of subgrid cloud variability on the grid-mean radiative fluxes. Although the effects of subgrid cloud variability on the radiative fluxes have been recognized by various observational, theoretical and diagnostic studies, the treatment of cloud distributions in the radiation schemes of GCMs still contains great uncertainties. In this study, we take a further step to isolate the individual contributions of cloud horizontal inhomogeneity and vertical overlap on domain-averaged radiative fluxes and heating rates. The diagnostic radiation calculation M2 is performed by replacing the cloud optical property of cloudy boxes with the in-cloud mean value over the CRM domain, which removed the cloud horizontal inhomogeneity. The comparison among the CRM, M2, and M1 shows that given the mean cloud optical properties and cloud fractions of CRM simulation, the cloud horizontal inhomogeneity and vertical overlap are equally important for producing accurate domain-averaged radiative fluxes and heating rates. In general, the removal of cloud inhomogeneity in the radiation calculation leads to smaller net TOA and SRF shortwave and longwave fluxes due to the larger net cloud effects, and also results in the smaller net radiative cooling throughout the troposphere. The use of the random overlap assumption also produces smaller net TOA and SRF shortwave fluxes but comparable TOA and larger SRF longwave fluxes averaged over the 30-day period during TOGA COARE. The effect of random overlap assumption on the net radiative heating rate is to enhance the net cooling above 8 km but to reduce the net cooling below.

The results presented in this study are from the CRM simulation of tropical cloud systems over the western Pacific Ocean. The analysis for midlatitude cloud systems simulated using the large-scale forcing from the Department of Energy (DOE) Atmospheric Radiation

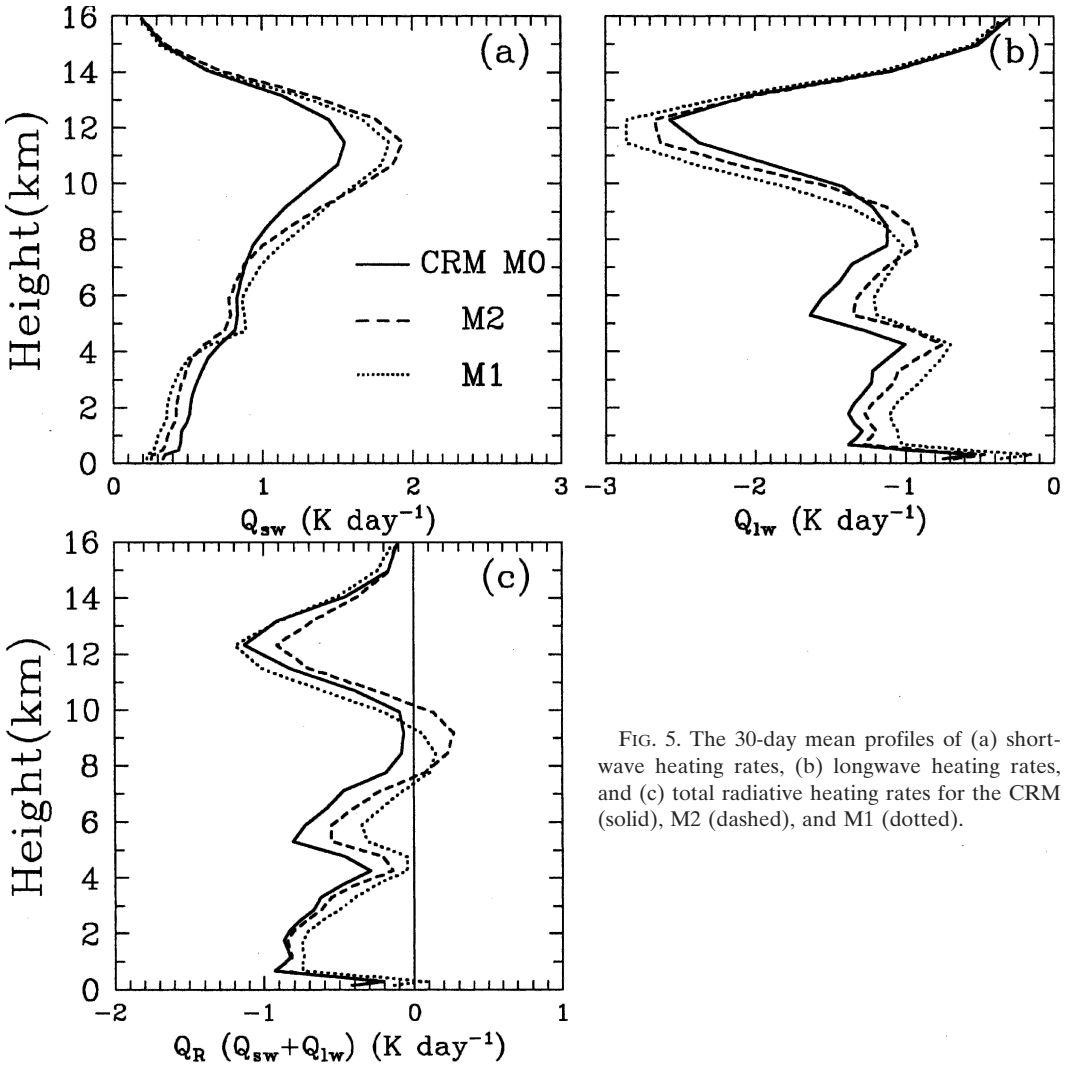

FIG. 5. The 30-day mean profiles of (a) shortwave heating rates, (b) longwave heating rates, and (c) total radiative heating rates for the CRM (solid), M2 (dashed), and M1 (dotted).

Measurement (ARM) program showed similar effects of subgrid cloud variability on the domain-averaged fluxes and heating rates (e.g., Wu and Liang 2003). There are increasing efforts to develop methods for incorporating both horizontal and vertical variability into GCM radiation parameterization schemes (e.g., Liang and Wang 1997; Li 2002; Stephens et al. 2004). The long-term cloud properties generated by the CRM together with temperature and moisture fields will be a useful test bed for evaluating these methods. The analysis presented in this paper is a diagnostic type of study and does not consider the feedbacks. Liang and Wang (1997) showed, by implementing the mosaic treatment in GCMs, the subgrid cloud variability strongly affects the climate simulation of temperature and cloud fields. There are growing efforts to embed the CRM directly into GCMs as a "superparameterization" (e.g., Grabowski 2001; Randall et al. 2003). With this framework, the two-way interaction of cloud and radiation can be investigated and its effects on the global circulation can be directly estimated (J. Cole 2004, personal communication).

Acknowledgments. This research was supported by the Biological and Environmental Research Program (BER), U.S. Department of Energy, Grant DE-FG03-02ER63354. Computing support by Daryl Herzmann is greatly appreciated. The comments of two anonymous reviewers help improve the presentation of the results. The views expressed are those of the authors and do not necessarily reflect those of the sponsoring agencies or the Illinois State Water Survey.

REFERENCES

Barker, H. W., 1996: A parameterization for computing grid-averaged solar fluxes for inhomogeneous marine boundary

layer clouds. Part I: Methodology and homogeneous biases. *J. Atmos. Sci.,* **53,** 2289–2303.

——, G. L. Stephens, and Q. Fu, 1999: The sensitivity of domain-averaged solar fluxes to assumptions about cloud geometry. *Quart. J. Roy. Meteor. Soc.,* **125,** 2127–2152.

Cahalan, R. F., W. Ridgway, W. J. Wiscombe, T. L. Bell, and J. B. Snider, 1994: The albedo of fractal stratocumulus clouds. *J. Atmos. Sci.,* **51,** 2434–2455.

Clark, T. L., W. D. Hall, and J. L. Coen, 1996: Source code documentation for the Clark-Hall cloud-scale model: Code version G3CH01. NCAR Tech. Note TN426+STR, 130 pp.

Fu, Q., M. C. Cribb, H. W. Barker, S. K. Krueger, and A. Grossman, 2000: Cloud geometry effects on atmospheric solar absorption. *J. Atmos. Sci.,* **57,** 1156–1168.

Gates, W. L., 1992: AMIP: The Atmospheric Model Intercomparison Project. *Bull. Amer. Meteor. Soc.,* **73,** 1962–1970.

Grabowski, W. W., 2001: Coupling cloud processes with the large-scale dynamics using the cloud-resolving convection parameterization (CRCP). *J. Atmos. Sci.,* **58,** 978–997.

Hahn, C. J., S. G. Warren, J. London, R. M. Chervin, and R. Jenne, 1982: Atlas of simultaneous occurrence of different cloud types over the ocean. NCAR Tech. Note TN-201+STR, 212 pp.

——, ——, ——, ——, and ——, 1984: Atlas of simultaneous occurrence of different cloud types over land. NCAR Tech. Note TN-241+STR, 216 pp.

Kessler, E., 1969: *On the Distribution and Continuity of Water Substance in Atmospheric Circulations*. *Meteor. Monogr.,* No. 32, Amer. Meteor. Soc., 84 pp.

Kiehl, J. T., J. J. Hack, G. B. Bonan, B. A. Boville, B. P. Briegleb, D. L. Williamson, and P. J. Rasch, 1996: Description of the NCAR Community Climate Model (CCM3). NCAR Tech. Note TN-420+STR, 160 pp. [Available online at http://www.cgd.ucar.edu/cms/ccm3/TN-420.]

Koenig, L. R., and F. W. Murray, 1976: Ice-bearing cumulus cloud evolution: Numerical simulation and general comparison against observations. *J. Appl. Meteor.,* **15,** 747–762.

Li, J., 2002: Accounting for unresolved clouds in a 1D infrared radiative transfer model. Part I: Solution for radiative transfer, including cloud scattering and overlap. *J. Atmos. Sci.,* **59,** 3302–3320.

——, and H. W. Barker, 2002: Accounting for unresolved clouds in a 1D infrared radiative transfer model. Part II: Horizontal variability of cloud water path. *J. Atmos. Sci.,* **59,** 3321–3339.

Liang, X.-Z., and W. C. Wang, 1997: Cloud overlap effects on general circulation model climate simulations. *J. Geophys. Res.,* **102,** 11 039–11 047.

Morcrette, J. J., and Y. Fouquart, 1986: The overlapping of cloud layers in shortwave radiation parameterization. *J. Atmos. Sci.,* **43,** 321–328.

Randall, D. A., M. F. Khairoutdinov, A. Arakawa, and W. W. Grabowski, 2003: Breaking the cloud parameterization deadlock. *Bull. Amer. Meteor. Soc.,* **84,** 1547–1564.

Stephens, G. L., 1984: The parameterization of radiation for numerical weather prediction and climate models. *Mon. Wea. Rev.,* **112,** 826–867.

——, P. M. Gabriel, and S.-C. Tsay, 1991: Statistical radiative transport in one-dimensional media and its application to the terrestrial atmosphere. *Trans. Theory Stat. Phys.,* **20,** 139–175.

——, N. B. Wood, and P. M. Gabriel, 2004: An assessment of the parameterization of subgrid-scale cloud effects on radiative transfer. Part I: Vertical overlap. *J. Atmos. Sci.,* **61,** 715–732.

Tian, L., and J. A. Curry, 1989: Cloud overlap statistics. *J. Geophys. Res.,* **94,** 9925–9935.

Wu, X., and M. W. Moncrieff, 2001: Long-term behavior of cloud systems in TOGA COARE and their interactions with radiative and surface processes. Part III: Effects on the energy budget and SST. *J. Atmos. Sci.,* **58,** 1155–1168.

——, and X.-Z. Liang, 2003: Month-long 2D cloud-resolving model simulation and resultant statistics of cloud systems over the ARM SGP. *Proc. 13th ARM Science Team Meeting*, Broomfield, CO, Department of Energy. [Available online at http://www.arm.gov/publications/proceedings/conf13/index.stm.]

——, W. W. Grabowski, and M. W. Moncrieff, 1998: Long-term behavior of cloud systems in TOGA COARE and their interactions with radiative and surface processes. Part I: Two-dimensional modeling study. *J. Atmos. Sci.,* **55,** 2693–2714.

——, W. D. Hall, W. W. Grabowski, M. W. Moncrieff, W. D. Collins, and J. T. Kiehl, 1999: Long-term behavior of cloud systems in TOGA COARE and their interactions with radiative and surface processes. Part II: Effects of ice microphysics on cloud-radiation interaction. *J. Atmos. Sci.,* **56,** 3177–3195.

——, M. W. Moncrieff, and X.-Z. Liang, 2002: Radiative effects of cloud inhomogeneity and geometric association identified from a monthlong cloud-resolving model simulation. Preprints, *11th Conf. on Atmospheric Radiation*, Ogden, UT, Amer. Meteor. Soc., J39–J40.

Xu, K.-M., 2005: The sensitivity of diagnostic radiative properties to cloud microphysics among cloud-resolving model simulations. *J. Atmos. Sci.,* **62,** 1241–1254.